Rip1 (Receptor-interacting protein kinase 1) mediates necroptosis and contributes to renal ischemia/reperfusion injury

Andreas Linkermann[1], Jan H. Bräsen[2], Nina Himmerkus[3], Shuya Liu[4,5], Tobias B. Huber[4], Ulrich Kunzendorf[1] and Stefan Krautwald[1]

[1]Division of Nephrology and Hypertension, Christian-Albrechts-University, Kiel, Germany; [2]Institute for Pathology, Christian-Albrechts-University, Kiel, Germany; [3]Institute of Physiology, Christian-Albrechts-University, Kiel, Germany; [4]Renal Division, University Hospital Freiburg, Freiburg, Germany and [5]Spemann Graduate School of Biology and Medicine, Albert-Ludwigs-University, Freiburg, Germany

Loss of kidney function in renal ischemia/reperfusion injury is due to programmed cell death, but the contribution of necroptosis, a newly discovered form of programmed necrosis, has not been evaluated. Here, we identified the presence of death receptor–mediated but caspase-independent cell death in murine tubular cells and characterized it as necroptosis by the addition of necrostatin-1, a highly specific receptor-interacting protein kinase 1 inhibitor. The detection of receptor-interacting protein kinase 1 and 3 in whole-kidney lysates and freshly isolated murine proximal tubules led us to investigate the contribution of necroptosis in a mouse model of renal ischemia/reperfusion injury. Treatment with necrostatin-1 reduced organ damage and renal failure, even when administered after reperfusion, resulting in a significant survival benefit in a model of lethal renal ischemia/ reperfusion injury. Unexpectedly, specific blockade of apoptosis by zVAD, a pan-caspase inhibitor, did not prevent the organ damage or the increase in urea and creatinine *in vivo* in renal ischemia/reperfusion injury. Thus, necroptosis is present and has functional relevance in the pathophysiological course of ischemic kidney injury and shows the predominance of necroptosis over apoptosis in this setting. Necrostatin-1 may have therapeutic potential to prevent and treat renal ischemia/reperfusion injury.

Correspondence: *Ulrich Kunzendorf, Division of Nephrology and Hypertension, Christian-Albrechts-University Kiel, Schittenhelmstrasse 12, Kiel 24105, Germany. E-mail: kunzendorf@nephro.uni-kiel.de*

Programmed cell death (PCD) was initially used synonymously with apoptosis until caspase-independent cell death (CICD) was discovered.[1,2] Cell shrinkage, chromatin condensation, membrane blebbing, and nuclear fragmentation are due to the proteolytic activity of caspases and define the characteristics of apoptosis[2] mediated via the extrinsic or the intrinsic apoptotic pathway.[3,4] The receptor-mediated extrinsic pathway involves the assembly of the death-inducing signaling complex, which includes death receptors (e.g., tumor necrosis factor receptor (TNFR), Fas), the adapter protein Fas-associated death domain, and the initiator caspase-8 that subsequently cleaves the effector caspase-3 to execute the apoptosis.[5] The intrinsic apoptotic pathway involves cytochrome *c* release from mitochondria,[5,6] which results in the assembly of the caspase-9-containing apoptosome, which, similar to caspase-8, activates caspase-3.[7] The apoptotic cascade is involved in innate immune responses targeting virally infected cells.[3] Consequently, viruses express caspase inhibitors such as the baculovirus protein p35 or the cowpox virus protein crmA.[8,9] Loss of caspase-8 or Fas-associated death domain, and also inhibition of caspase-8 by the pan-caspase inhibitor zVAD or viral proteins, results in necroptosis, which is a specific subform of programmed necrosis. Programmed necrosis encompasses different signaling pathways other than necroptosis, e.g., programmed necrosis mediated by lysosomal membrane peroxidation or the release of necrosis-inducing factors after mitochondrial permeability transition (MPT).[10–12] Execution of necroptosis requires the assembly of the receptor-interacting protein kinase (RIP)1- and/or RIP3-containing necroptosome.[13–16] Other authors define necroptosis as CICD with a necrotic phenotype that can be prevented by the highly specific Rip1 inhibitor necrostatin-1 (Nec-1).[17,18] In this article, we use the latter definition of necroptosis.

Physiologically relevant necroptosis has been demonstrated to occur in T lymphocytes,[19,20] photoreceptors,[21] a stroke model,[22] and has been suggested to contribute to the pathogenesis of myocardial infarction.[23] In addition, it has been interpreted as a second-line defense mechanism against

viruses because infection with a sublethal dose of vaccinia virus led to 100% lethality of RIP3-deficient mice.[10] Importantly, the lethal phenotype of caspase-8-deficient mice[24] was recently demonstrated to be mediated via the necroptosome, further underlining both the *in vivo* relevance and the current concept of necroptosis.[25,26] In line with this report, conditional targeting of Fas-associated death domain in gastrointestinal epithelial cells causes severe colitis, a phenotype that can be reversed on a RIP3-deficient background.[27]

In renal ischemia/reperfusion (IR) models, a multiplicity of studies have investigated the influence of defined components of the machinery involved in PCD.[28] Lymphocytes, natural killer cells, and macrophages have been demonstrated to significantly contribute to tubular cell PCD.[29–32] Conflicting results exist with regard to the influence of members of the TNF superfamily. Although Fas-mutated *lpr* mice are protected from renal IR injury (IRI),[33,34] the protective trend in immunodeficient mice that were adoptively transferred with natural killer cells taken from Fas ligand (FasL)–mutated *gld* mice did not reach statistical significance.[29] In contrast, one recent report demonstrated a protective effect in *gld* mice with renal IRI.[35] Importantly, both TNF-α and FasL are capable of inducing necroptosis *in vivo*,[25,26] suggesting that the studies on *gld* or *lpr* mice and TNFR mutants do not provide a tool to discriminate between apoptosis and necroptosis.

Here we demonstrate the functional relevance of necroptosis in the kidney. Importantly, in comparison with zVAD treatment, the protective effect of Nec-1 was more pronounced, which suggests for a functional predominance of necroptosis over apoptosis in the pathophysiology of renal IRI.

RESULTS
Renal tubular cells are insensitive to Fas- or TNF-α-mediated apoptosis

We investigated the mechanisms of PCD in the murine tubular cell line TKPTS. As demonstrated in Figure 1a, incubation with vehicle, 100 ng/ml TNF-α, or activating α-Fas monoclonal antibodies did not cause significant cell death as detected by annexin V positivity after 24 h of incubation at 37 °C. For comparison, Jurkat cells, a T-cell line sensitive for Fas-mediated apoptosis, were stimulated for 5 h at 37 °C with the indicated reagents.

Renal tubular cells are sensitive to TNFα/cycloheximide (CHX)-mediated CICD

Induction of TNF-α-mediated apoptosis requires the additional application of CHX in some cells.[1] We added 2 μg/ml CHX to TNF-α-treated TKPTS cells and investigated annexin V positivity 24 h later (Figure 1b). Again, Jurkat T cells are depicted for comparison. Although the addition of the pan-caspase inhibitor zVAD prevented caspase-dependent, TNF-α/CHX-induced apoptotic cell death in Jurkat cells, no reduction of annexin V positivity was measured in TKPTS cells.
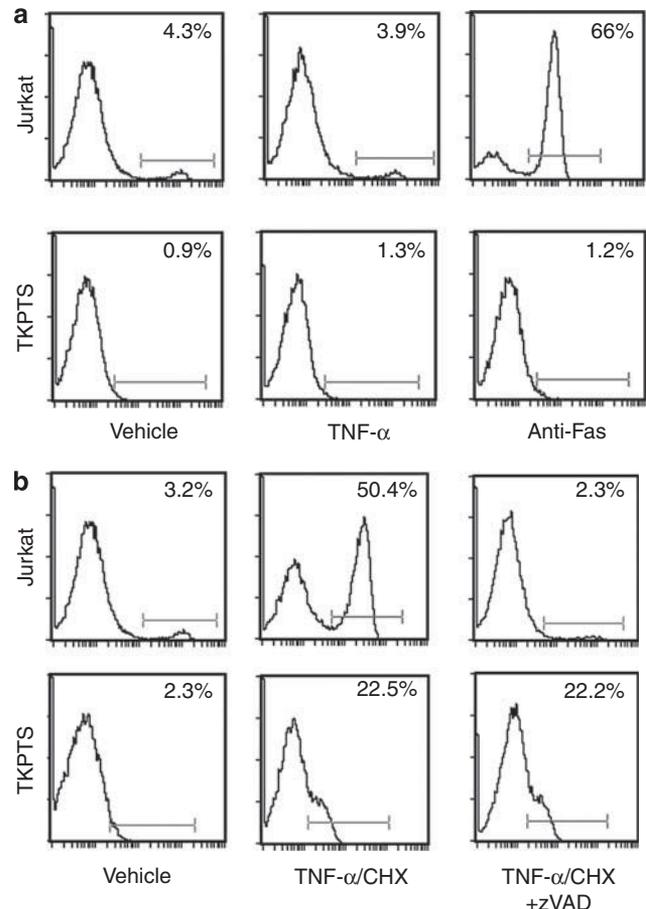

Figure 1 | TKPTS cells are insensitive to death receptor–mediated apoptosis and sensitive to death receptor–mediated caspase-independent cell death (CICD). (**a**) Jurkat T cells and TKPTS cells were treated with vehicle, activating α-Fas monoclonal antibodies, or tumor necrosis factor alpha (TNF-α) for 5 h, as indicated. Positivity for annexin V was detected by fluorescence-activated cell sorting analysis. (**b**) Jurkat T cells and TKPTS cells were treated with vehicle or TNF-α + cycloheximide (CHX) in the presence or absence of the pan-caspase inhibitor zVAD and stained for annexin V positivity after 5 or 24 h, respectively.

TNF-α-mediated necroptosis in the renal proximal tubular (prox. tubule) cell line TKPTS is mediated by Rip1

To further classify the CICD that TKPTS cells undergo in Figure 1b, we investigated the recently described necroptosis pathway.[14,16] Annexin V positivity is an established readout for both apoptotic and necroptotic cell death and allows to distinguish between apoptosis, programmed necrosis, and necroptosis only through the addition of zVAD and Nec-1.[13] Classical assays for necroptosis include the stimulation of cells with a combination of TNF-α, CHX, and zVAD (herein denoted as TCZ).[10] Annexin V positivity increased from 2.07% in the vehicle-treated cells to 20.19% in the TCZ-stimulated cells. The significant decrease in annexin V positivity upon additional treatment with Nec-1 (9.11%, $P < 0.05$) defines this subform of CICD as Rip1-dependent necroptosis (Figure 2b). For comparison, similar experiments
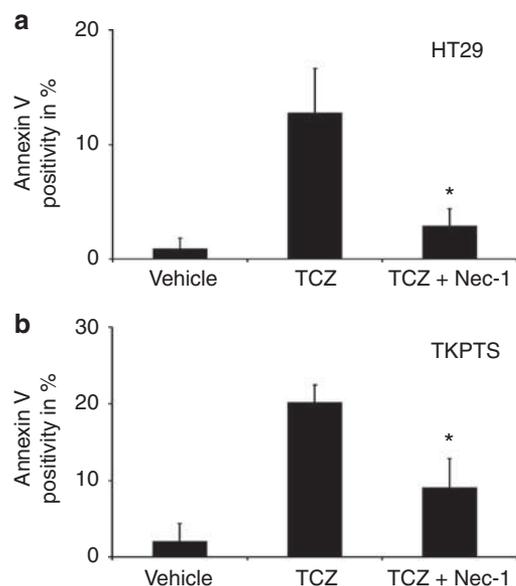
Figure 2 | **Tumor necrosis factor alpha (TNF-α)-mediated necroptosis in TKPTS cells is prevented by the addition of necrostatin-1 (Nec-1).** (**a**) Caspase-independent cell death of HT29 cells (positive control) was induced by the combined treatment of TNF-α/cycloheximide (CHX)/zVAD (TCZ) for 5 h and identified as necroptosis by the lack of annexin V positivity in the presence of the specific receptor-interacting protein kinase 1 (Rip1) inhibitor Nec-1 ($P < 0.05$). (**b**) TKPTS cells were treated as described in Figure 1a for 24 h, and annexin V positivity was determined by fluorescence-activated cell sorting analysis. Four independent experiments were conducted. *$P < 0.05$.

Figure 3 | **In contrast to the murine mesangial cell line MMC, the glomerular endothelial cell line glEND is susceptible to necroptosis.** (**a**) Lysates prepared from the murine standard necroptosis-sensitive cell line L929 (fibroblasts), the glomerular endothelial cell line glEND, and the murine mesangial cell line MMC were analyzed for the expression of receptor-interacting protein kinase 1 (RIP)1 and RIP3. Expression of β-actin served as a loading control. (**b**) The abovementioned cell lines were cultivated for 4 h (L929) or 24 h in the presence or absence of tumor necrosis factor alpha (TNF-α)/cycloheximide (CHX)/zVAD (TCZ) and necrostatin-1 (Nec-1) as indicated. Similar to L929 cells, glEND cells were susceptible to necroptosis, whereas MMCs were not. Data from three independent experiments are shown. *$P < 0.05$.

using HT29 cells, a necroptosis-sensitive cell line,[11] are shown (Figure 2a). Experiments were repeated four times. To further specify the dependence of necroptosis on Rip1, we co-incubated TKPTS cells with Rip1-specific siRNA for 48 h before TCZ treatment. As demonstrated in Supplementary Figure S1 online, knockdown of Rip1 reduced necroptosis in this setting. However, we were unable to co-precipitate Rip1 and Rip3 in these cells. To exclude the presence of apoptosis, we stimulated TKPTS cells with a combination of TNF-α, CHX, and zVAD, and investigated the presence of cleaved caspase-3 and compared those with Jurkat cells. Supplementary Figure S2 online demonstrates the absence of caspase-3 activation in TKPTS cells after 4 or 24 h. Taken together, these results provide the first evidence of necroptosis in kidney cells.

In contrast to murine mesangial cells, murine glomerular endothelial cells are sensitive to TNF-α-mediated necroptosis
To evaluate the susceptibility of other kidney cells to undergo necroptosis, we investigated Rip1 and Rip3 expression levels in the murine glomerular endothelial cell line glENDp54 and the murine mesangial cell line MMC. For comparison, the commonly used necroptosis-sensitive cell line L929 (murine fibroblasts) was investigated. Rip1 and Rip3 were detected in all of these cell lines, although RIP3 expression in MMCs was significantly lower than in the glENDp54 and L929 cells. Detection of β-actin served as a loading control (Figure 3a).
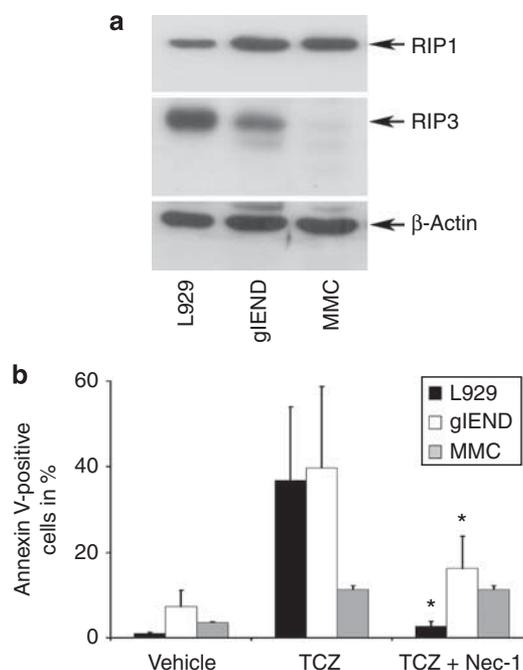
Sensitivity to necroptosis was further tested by stimulation of each cell line with TCZ and TCZ + Nec-1 as indicated (Figure 3b), after treatment for 24 h in the case of MMCs and glENDs and 5 h in the case of L929 cells. Although cell death in MMCs was not induced upon stimulation with TCZ, glENDs showed a delayed similar reaction pattern when compared with L929 cells after TCZ stimulation. The CICD in L929 cells and glENDs can be defined as necroptosis because of the significant reduction upon addition of Nec-1. In addition, we knocked down RIP3 by siRNA 48 h before CICD and demonstrated the protection from necroptosis in glENDs (Supplementary Figure S3 online). To analyze the PCD susceptibility of podocytes, we analyzed PCD in a widely used human podocyte cell line. Upon stimulation with either vehicle, TNF-α, TNFα/CHX, and TNF-α/CHX/zVAD for 24 h, no significant induction of annexin V positivity was observed (Supplementary Figure S4 online).

Detection of Rip1 and Rip3 expression in freshly isolated kidney tissues
To investigate the *in vivo* presence of the molecular machinery that has been demonstrated to be required for the execution of necroptosis, we generated lysates of homogenized murine whole-kidney tissue, freshly isolated thick
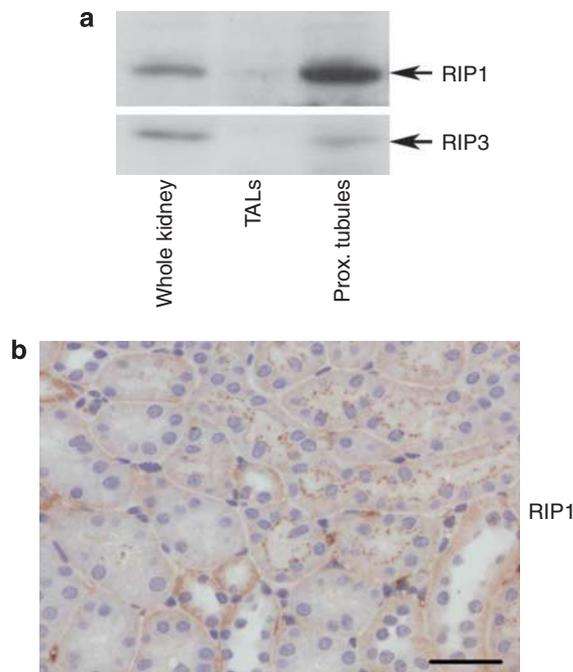
Figure 4 | Detection of the protein machinery required for necroptosis in renal tubular cells. (a) Protein expression of the necroptosis key factors Rip1 (receptor-interacting protein kinase 1) and RIP3 was detected in lysates prepared from whole-untreated murine kidneys, freshly isolated renal thick ascending limb segments (TALs), or freshly isolated proximal tubules (prox. tubules), as indicated. (b) Detection of Rip1 by immunohistochemistry in kidney sections of an untreated C57BL/6N mouse in the basolateral tubular compartment and in the brush border of tubular cells. Bar = 20 μm.

ascending limb segments, and freshly isolated renal proximal tubules (prox. tubules). Western blot analyses using antibodies against Rip1 and Rip3 were performed to demonstrate protein expression levels (Figure 4a). Note that the thick ascending limb lane was loaded with 8 μg protein, whereas the whole kidney and the prox. tubule lanes each were loaded with 40 μg protein. In kidney slices taken from untreated mice, immunohistochemistry-based determination of basal levels of Rip1 was performed (Figure 4b) as recently described.[36] Cytosolic expression of Rip1 was located toward the basolateral compartment of tubular cells. In addition, Rip1 expression was found close to the brush border. Adequate antibodies for immunohistochemical detection of murine RIP3 have not been established to our knowledge.

Inhibition of Rip1-mediated necroptosis by necrostatin-1 protects from renal ischemia/reperfusion injury

To evaluate the functional relevance of Rip1-mediated necroptotic cell death in an appropriate *in vivo* model of acute renal failure, we used the well-established renal IR model. Six- to eight-week-old male C57BL/6N mice underwent bilateral renal pedicle clamping for 30 min, followed by 48 h of reperfusion. Mice were left untreated, underwent sham, or IR surgery, and received 200 μl phosphate-buffered saline or 1.65 mg Nec-1/kg body weight in a total volume of

200 μl intraperitoneally at 15 min before the onset of ischemia. Kidneys were harvested for histological evaluation, and blood samples were used for the determination of serum concentrations of urea and creatinine. Periodic acid–Schiff staining was performed, and a renal damage score was used, as previously published.[37] Representative kidney sections are shown in Figure 5a, and results of the evaluation of the renal damage score are shown in Figure 5b. Marked reduction of renal damage was achieved by a single application of Nec-1 ($P < 0.05$). Electron microscopy detected necrotic cells in renal tubules from untreated, sham-operated, and IR-treated mice in the presence or absence of Nec-1. Representative sections are depicted in Figure 5c. Hallmarks of necrotic cell death such as nuclear swelling, loss of mitochondria, and loss of cell organelle content predominantly appeared in the IR-treated group (Supplementary Figure S5 online). Typical hallmarks of apoptotic cell death such as blebbing and shrinkage of cells have not been detected. As demonstrated in Figure 5d and e, in untreated or sham-operated mice that were followed up for 48 h of reperfusion, the basal serum urea levels were at 44.25 ± 5.7 mg/dl. The basal levels of serum creatinine values did not exceed 0.11 mg/dl (0.10 ± 0.01 mg/dl). As expected, IR-treated mice showed increased blood levels of urea and creatinine at that time point, but also 24 and 72 h after reperfusion. Statistically significant reduction of serum urea and serum creatinine levels was detected at all of these three time points after reperfusion. To further confirm the specificity of Nec-1 to interfere with Rip1, we used an inactive derivative of necrostatin-1 (Nec-1i) that did not influence serum concentrations of urea and creatinine (Supplementary Figure S6 online). These experiments provide the first evidence for the presence of necroptosis in a pathophysiologically relevant process in the kidney.

Therapeutical potential of necrostatin-1 in renal ischemia–reperfusion

To further characterize the time course of necroptosis in renal IRI, we investigated the therapeutical potential of Nec-1 when applied 15 min after reperfusion. Thus, mice underwent IR surgery for 30 min without preoperative injections but were injected with 200 μl phosphate-buffered saline or an equal volume containing 1.65 mg Nec-1/kg body weight 15 min after reperfusion. After 48 h, the mice were killed, blood samples were taken, and kidneys were harvested for histological evaluation. Representative kidney sections are demonstrated in Figure 6a, and a quantification of renal damage is shown in Figure 6b. The reduction of renal damage by Nec-1 15 min after reperfusion was comparable to the results obtained with Nec-1 pretreatment (Figure 5b) before the onset of ischemia ($P < 0.05$). Nec-1 induced a significant reduction in serum creatinine values (Figure 6d, $P < 0.05$), but the reduction of serum urea levels did not reach statistical significance (Figure 6c). However, urea levels were not significantly different from those obtained with Nec-1 treatment before pedicle clipping (Figure 5d). In a separate experiment, a high-dose application of Nec-1 was investigated
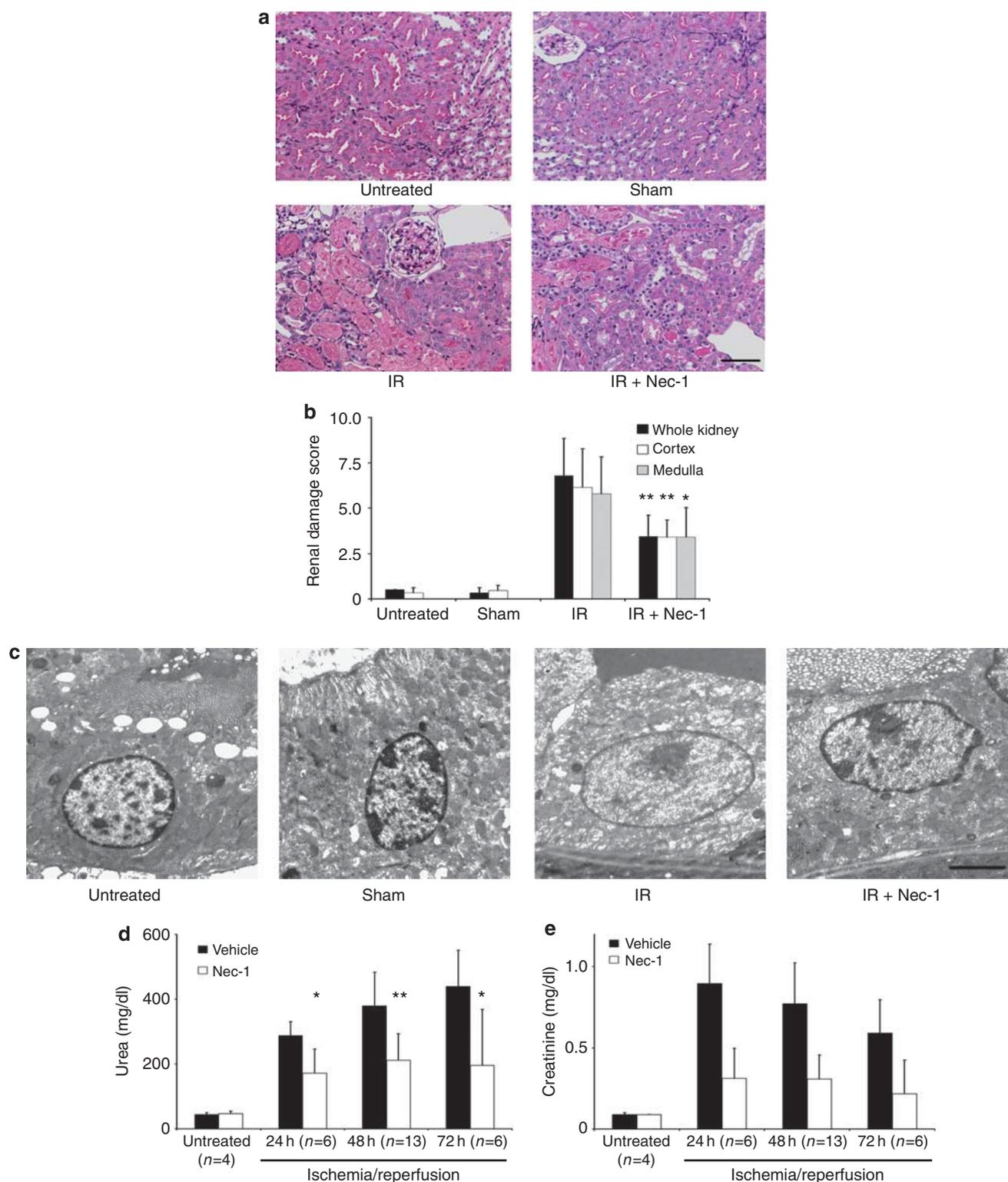
Figure 5 | Necroptosis essentially contributes to renal ischemia/reperfusion injury *in vivo*. Six- to eight-week-old male C57BL/6N mice were treated with a 200 μl total volume of phosphate-buffered saline or necrostatin-1 (Nec-1) 15 min before sham surgery or bilateral renal pedicle clipping for 30 min, followed by 48 h of reperfusion, as indicated. (a) Representative Periodic acid–Schiff-stained kidney sections are illustrated. (b) Quantification of the renal tubular damage is demonstrated for whole kidneys (black bars), the outer renal cortex (white bars), and the medullary cortex (gray bars). Bar = 20 μm. (c) Representative electron micrographs of necrotic proximal renal tubule (prox. tubule) cells are shown. Note the prominent nuclear swelling, loss of nuclear condensation, and loss of mitochondrial and endoplasmatic reticulum mass as hallmarks of programmed necrosis. Bar = 2 μm. For each of the abovementioned groups, and for completely independent groups that have been analyzed 24 and 72 h after reperfusion, respectively, serum concentrations of urea (d) and creatinine (e) are depicted (*P*-values are: * <0.05, ** <0.01).
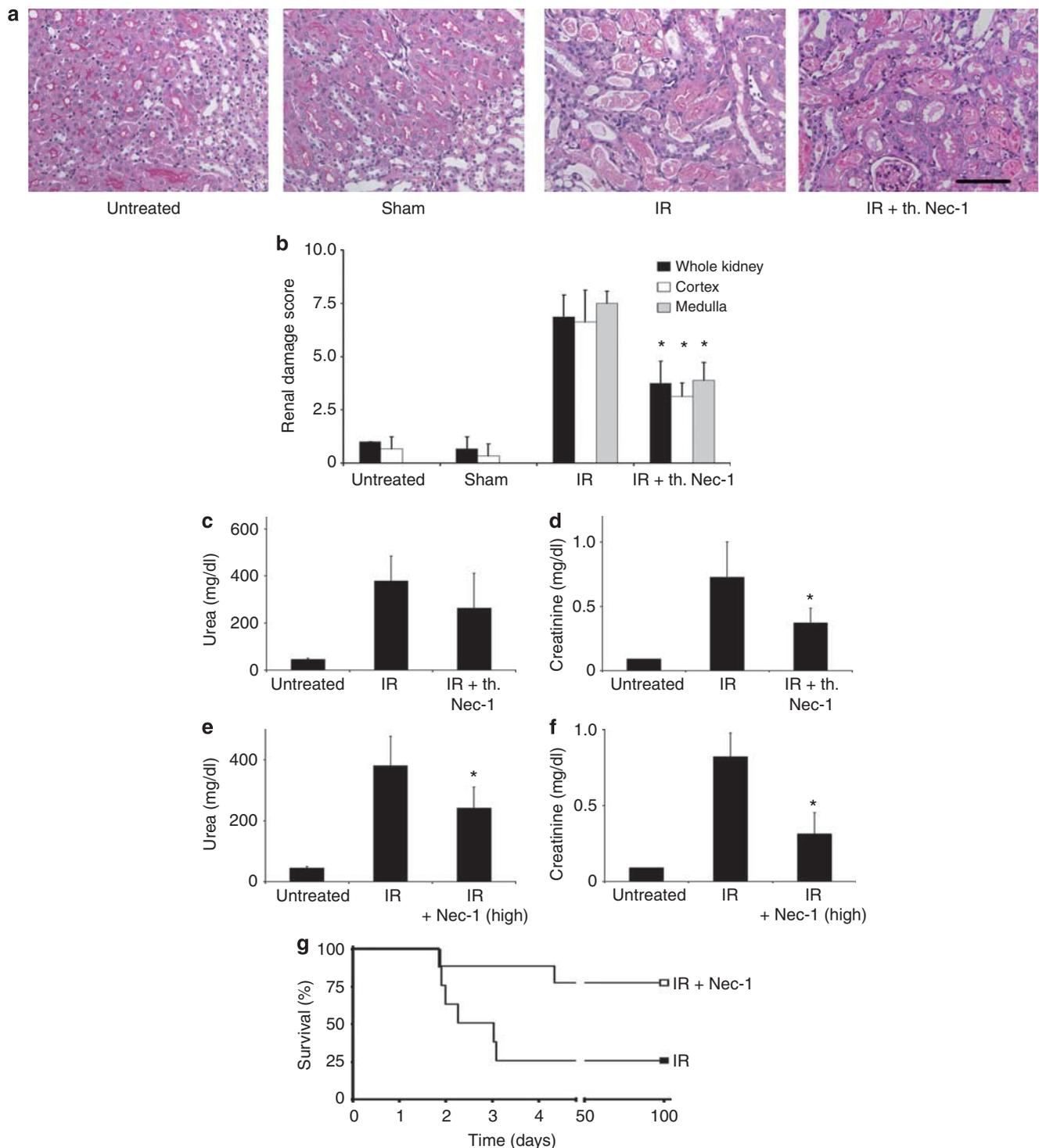
Figure 6 | Therapeutical potential of necrostatin-1 in renal ischemia/reperfusion injury (IRI). Six- to eight-week-old male C57BL/6N mice were left untreated or underwent sham surgery or 30 min of bilateral renal pedicle clipping, followed by 48 h of reperfusion with or without the application of 200 μl phosphate-buffered saline or therapeutical necrostatin-1 (Nec-1) (th. Nec-1) 15 min after reperfusion, as indicated. (**a**) Representative periodic acid–Schiff-stained kidney sections are shown. Bar = 20 μm. (**b**) Renal tubular damage scores of these organs were quantified. Levels of urea and creatinine were determined in serum samples taken at 48 h after reperfusion and are depicted in **c** and **d**, respectively ($n = 8$ for each group). In a separate experiment, multiple doses of Nec-1 (four applications within 240 min after reperfusion, see text for details) did not provide an additional protective effect on serum concentrations of urea (**e**) or creatinine (**f**) ($n = 5$ for each group) when compared with Figure 5. (**g**) In a model of lethal renal IRI (40 min of bilateral pedicle clamping), mice received either two injections of 200 μl phosphate-buffered saline (black squares) or two applications of 1.65 mg Nec-1/kg body weight (white squares) intraperitoneally, 15 min before ischemia and 15 min after reperfusion. Survival statistics are demonstrated in a Kaplan–Meier plot ($n = 10$ for each group, $P < 0.01$). *$P < 0.05$.

for putatively additive effects. Mice received injections of 1.65 mg Nec-1/kg body weight for four times (15 min before ischemia and 15, 120, and 240 min after reperfusion). As demonstrated in Figure 6e and f, no additive protective effect was observed for multiple doses of Nec-1 when compared with the data from Figure 5d and e.

Necrostatin-1 prolongs survival after otherwise lethal renal ischemia/reperfusion injury

To further analyze the potency of Nec-1 in reducing renal IRI, we challenged the Rip1 inhibitor in a 40-min bilateral clipping model of renal ischemia that is characterized by high mortality in C57BL/6N mice. As demonstrated in Figure 6g, two applications of 1.65 mg Nec-1/kg body weight in 200 μl total volume that were applied 15 min before ischemia onset and 15 min after the onset of reperfusion led to a significant difference in overall survival when compared with phosphate-buffered saline-treated mice in this model ($P < 0.05$, $n = 10$).

Renal IRI pathophysiologically occurs predominantly through necroptosis rather than apoptosis

Because the blockade of apoptosis with the pan-caspase inhibitor zVAD has been suggested to prevent renal injury after IR,[38] and because we wanted to understand the contribution of each single PCD component in this setting, we investigated the effects of blocking apoptosis and necroptosis. We therefore compared the amount of protection detected in Nec-1-treated mice (the experimental setup was described in Figure 5) with an additional group that was treated with 10 mg zVAD/kg body weight in an equal final volume of 200 μl 15 min before the induction of ischemia. Representative Periodic acid–Schiff-stained kidney sections taken 48 h after reperfusion are demonstrated for untreated, IR, IR + Nec-1, and IR + zVAD groups in Figure 7a, and a quantification of renal damage is depicted in Figure 7b. Interestingly, in the zVAD-treated group, no reduction of serum urea levels was detected, and the reducing trend in serum creatinine levels did not reach statistical significance (Figure 7c and d). Consistent with the high numbers of necrotic tubular cells, we concluded that necroptosis, rather than apoptosis, accounts for significant tubular damage in renal IRI.

DISCUSSION

Changes in histomicrographs taken of kidneys after acute renal IRI were specified by pathologists as acute tubular necrosis for years before the first description of apoptosis in renal IRI in 1992.[39] Since then, among nephrologists, a dogma developed that presumes that the genetically programmed and putatively therapeutically alterable fraction of cells that undergo PCD in renal IRI is limited to apoptotic cells. Extrinsic apoptosis has been established to be initiated by death receptors that are members of the TNFR superfamily of transmembrane proteins,[3,40] and various reports discussed the *in vivo* relevance of TNFR family members in

the kidney.[34,37] Because recent data substantially contributed to our understanding of the regulation of the molecular machinery involved in signaling events downstream of the TNFR and Fas, it has become clear that either apoptosis or necroptosis can be initiated by these receptors, depending on the intracellular status of the target cell. In the presence of an active caspase-8/FLIP$_L$ heterodimer, Rip1 is inactivated and necroptotic signaling is prevented.[26,41] If any single component of this heterodimer is lacking, uncleaved Rip1 will initiate the assembly of the necroptosome, which is believed to be responsible for the execution of necroptosis.[13,14,42] Therefore, previously conducted studies on *lpr*- or *gld*-mice[33,35] will not allow extrinsic apoptosis to be differentiated from necroptosis. Given these data and the finding that TNFR1-deficient mice are not protected from renal IRI,[43] we question the evidence for the functional contribution of apoptosis in this setting. Caspase-8-deficient mice are not viable,[24] and therefore cannot contribute to answering this question. Similarly, caspase-3 deficiency leads to early death of the mice at the age of 1 to 3 weeks.[44] Fas-associated death domain-deficient mice die during mid-gestational stages.[45,46] One report used zVAD and described a protective effect for caspase inhibition in renal IRI, but the authors do not provide data concerning the standard Periodic acid–Schiff staining for evaluation and quantification of renal damage or data for the serum levels of creatinine.[38] Furthermore, for the detection of apoptosis, TUNEL assays were performed that have been demonstrated to lack specificity when different cell death pathways are compared.[47] However, in our experiments, the same dose of zVAD did not reduce the serum levels of urea and creatinine and did not prevent organ damage (Figure 7). The incongruence might partly be explained by the different timing of the zVAD application.

In addition to death receptor–mediated extrinsic apoptosis, it has been suggested that the pathophysiology of renal IRI involves intrinsic apoptotic pathway activation as a consequence of cytochrome *c* release, caspase-9 cleavage, and Apaf-1 recruitment, which result in the formation of the apoptosome,[48] but to the best of our knowledge neither Apaf-1- nor caspase-9-deficient mice have been investigated in renal IRI. Our data concerning zVAD indicate that intrinsic apoptosis does not significantly contribute to the observed increase in serum levels of urea or creatinine or renal organ damage. Undoubtedly, there is an apoptotic component in the pathophysiological course of renal IRI that still might contribute to organ damage, but our data indicate a functional predominance of necroptosis over apoptosis in the deterioration of acute ischemic kidney failure.

Besides apoptosis and necroptosis, other types of PCD are likely to be involved, as even with high doses of Nec-1, substantial renal tubular damage was detected, although the serum levels of urea and creatinine were low (Figure 6). An obvious example is the release of apoptosis-inducing factor and the cleavage of poly [ADP-ribose] polymerase-1 upon severe renal ischemia as a consequence of persistent MPT, which leads to CICD in renal IRI.[48] Similarly, genetic
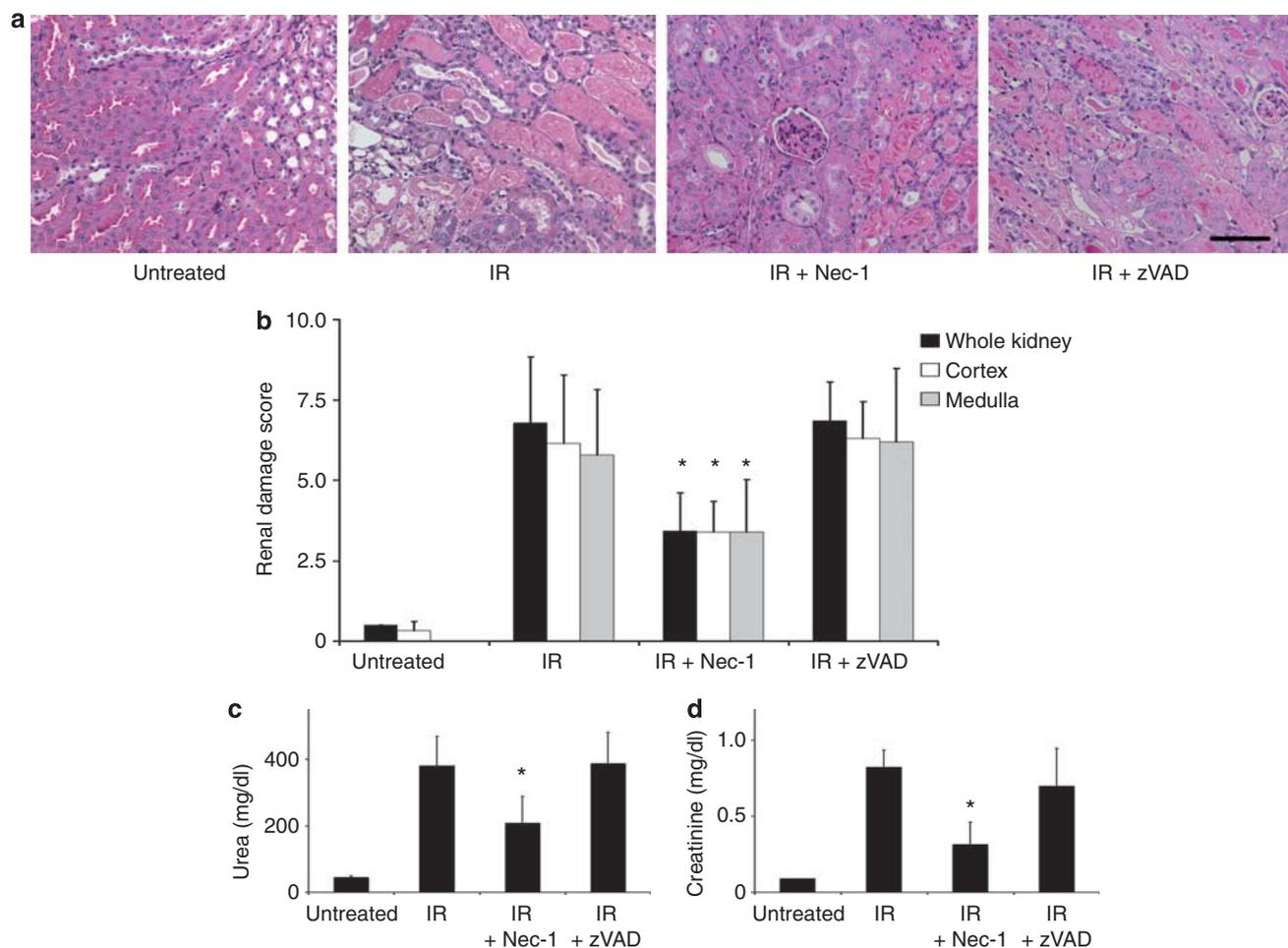
Figure 7 | Renal ischemia/reperfusion injury (IRI) is predominated by necroptosis rather than apoptosis. Six- to eight-week-old male C57BL/6N mice were left untreated or underwent 30 min of bilateral renal pedicle clipping in the presence of 200 μl phosphate-buffered saline, necrostatin-1 (Nec-1), or zVAD, as indicated. (**a**) Periodic acid-Schiff staining of representative renal histomicrographs is shown. Bar = 20 μm. (**b**) Quantification of the renal damage score is illustrated for whole kidneys (black bars), the outer renal cortex (white bars), and the medullary cortex (gray bars), as indicated. (**c**) Serum urea and (**d**) serum creatinine levels are depicted for all groups ($n = 8$ for each group, $P < 0.02$). *$P < 0.05$.

deficiency of the MPT pore (MPTP) regulator cyclophilin D is well established to protect against renal IRI.[49] In this regard, it has been discussed that the formation of the necroptosome might be an upstream event that results in opening of the MPTP and the subsequent MPT.[16] However, at least in activated cyclophilin D/RIP3 double-deficient T cells, this appears not to be the case.[20]

Given the protective effect of Nec-1 and the finding that TNFR1-deficient mice are not protected from renal IRI,[43] the most likely candidate to be responsible for death receptor–mediated necroptosis is the Fas–FasL system. Indeed, a recent report and our own unpublished observations indicate that inhibitory α-FasL monoclonal antibodies (MFL3 or MFL4) efficiently protect mice from renal IRI.[35] Because we demonstrate here that the apoptotic cascade is of minor importance in renal IRI (Figure 7), it might be speculated that FasL-mediated necroptosis is the deteriorating pathophysiological component, but data that support this

hypothesis are still lacking. However, we cannot rule out the possibility of death receptor–independent activation of the necroptosome under ischemic conditions, although in an attempt to define cell death subroutines the Nomenclature Committee on Cell Death suggested that necroptosis is death receptor–mediated.[47] Most studies on necroptosis have been conducted in a setting that involves TNFR stimulation using mouse fibroblast cell lines (L929 cells) that were stimulated with TNF-α. However, receptor-independent Rip1-dependent necroptosis has recently been reported, which might result from the assembly of the so-called ripoptosome.[50–52] This large 2 MDa complex is capable of inducing both apoptotic and necroptotic signals, but because Nec-1 does and zVAD does not protect from renal IRI, only ripoptosome-mediated necroptosis might be considered as a cause of renal IRI. Therefore, further investigations are required to unravel the precise characteristics of the necroptotic events in renal IRI. Blocking IR-induced necroptosis might be relevant in

kidney transplantation to maintain initial graft function, but also to avoid the triggers of acute and chronic rejection.

In conclusion, we describe both the presence and the functional relevance of Rip1-dependent necroptosis in the pathophysiology of renal IRI. Our results regarding the potency of Nec-1 to specifically interrupt necroptotic signaling provide a new strategy to prevent and treat ischemic kidney injury. Above that, the recognition of necrosis as a regulated process mandates reexamination of PCD in the kidney.

MATERIALS AND METHODS
Reagents and antibodies
The zVAD-fmk (herein referred to as zVAD), the ApoAlert annexin V-FITC antibody, the mouse α-Fas antibody (clone Jo2), and the mouse α-Rip1 antibody for western blotting were purchased from BD Biosciences (Heidelberg, Germany). The human α-Fas antibody (clone 7C11) was purchased from Immunotech (Marseille, France). Purified murine TNF-α was obtained from BioLegend (Uithoorn, the Netherlands). The reagents CHX and necrostatin-1 were obtained from Sigma-Aldrich (Taufkirchen, Germany). The inactive necrostatin-1–derivative Nec-1i was obtained from Calbiochem (Darmstadt, Germany). The polyclonal antibody against murine RIP3 was purchased from IMGENEX (Biomol, Hamburg, Germany). The β-actin antibody was purchased from Cell Signaling (Frankfurt, Germany), and the Rip1 antibody for immunohistochemistry was purchased from Santa Cruz (Heidelberg, Germany).

Cell culture
L929 fibrosarcoma cells and HT29 human adenocarcinoma cells were originally obtained from ATCC (Manassas, VA). L929 cells were cultured in Dulbecco's modified Eagle's medium (Invitrogen, Darmstadt, Germany) supplemented with 10% fetal calf serum (FCS) and penicillin-streptomycin. HT29 cells were maintained in Minimum essential medium with Earle's salts (Invitrogen), 10% FCS with glutamine, penicillin-streptomycin, nonessential amino acids, and sodium pyruvate. TKPTS cells were published previously[53] and were a kind gift from Bello-Reuss and Megyesi. TKPTS cells were cultured in Dulbecco's modified Eagle's medium/Ham's F12 medium with glutamine supplemented with SITE liquid media (Sigma-Aldrich), 15 mmol/l HEPES, 7% FCS, and penicillin-streptomycin. The murine mesangial cell line MMC was cultured in Dulbecco's modified Eagle's medium supplemented with 10% FCS, 63 U of bovine insulin (Sigma-Aldrich) per 500 ml medium, and penicillin-streptomycin. The murine glomerular epithelial cell line glENDp54 was cultured in RPMI 1640 containing 10% FCS and penicillin-streptomycin. All cell lines were cultured in a humidified 5% CO_2 atmosphere.

Assessment of cell death
Phosphatidylserine exposure to the outer cell membrane was quantified by annexin V staining followed by fluorescence-activated cell sorting analysis. Cells were stimulated for the indicated times at 37°C with 100 ng/ml TNF-α, 2 μg/ml CHX, 30 μmol/l Nec-1, or 25 μmol/l zVAD as indicated. Annexin V staining was performed according to the manufacturer's instructions. Fluorescence was analyzed using an EPICS XL (Beckman Coulter, Krefeld, Germany) flow cytometer. Data were analyzed using the EPICS System II software.

Induction of renal IRI
For all IRI experiments, 6- to 8-week-old male C57BL/6N mice (Charles River, Sulzfeld, Germany) were used. All *in vivo* experiments were conducted according to the protocols approved by the Protection of Animals Act. Induction of kidney IRI was performed as described previously.[54] Briefly, we performed a midline abdominal incision and a bilateral renal pedicle clipping for 30 min using microaneurysm clamps (Aesculab, Tuttlingen, Germany). Throughout the surgical procedure, the body temperature was maintained between 35 and 37.5°C by continuous monitoring using a temperature-controlled self-regulated heating system (Fine Science Tools, Heidelberg, Germany). After removal of the clamps, reperfusion of the kidneys was visually confirmed. The abdomen was closed in two layers using standard 6-0 sutures. Sham-operated mice received identical surgical procedures, except that microaneurysm clamps were not applied. To maintain fluid balance, all of the mice were supplemented with 1 ml of prewarmed phosphate-buffered saline administered intraperitoneally directly after surgery. The mice were killed 48 h after reperfusion if not otherwise specified for each experiment.

Isolation of renal prox. tubule and thick ascending limb segments
For detection of RIP expression, animals were killed 15 min after ischemia, followed by kidney isolation and enzymatic digestion. Sorting of prox. tubules and thick ascending limb segments according to their shape and morphology was performed at 4°C using a dissection microscope (Leica MZ16, Solms, Germany) in the presence of 1 mg/ml albumin as described previously.[37]

Histology, immunohistochemistry, and electron microscopy
Organs were dissected as indicated in each experiment and infused with 4% neutral-buffered formaldehyde, fixated for 48 h, dehydrated in a graded ethanol series and xylene, and finally embedded in paraffin. Paraffin sections (3–5 μm) were stained with periodic acid–Schiff reagent, according to the standard routine protocol. Immunohistochemistry for Rip1 was performed as described previously at a dilution of 1:500.[36] Stained sections were analyzed using an Axio Imager microscope (Zeiss, Oberkochen, Germany) at ×400 original magnification. Micrographs were digitalized using an AxioCam MRm Rev. 3 FireWire camera and AxioVision Rel. 4.5 software (Zeiss). Organ damage was quantified by an experienced pathologist in a double-blind manner on a scale ranging from 0 (unaffected tissue) to 10 (severe organ damage).

For ultrastructural analysis by electron microscopy, kidneys were dissected into small samples (1 mm sized), fixed in 2.5% glutaraldehyde in 0.1 mol/l sodium cacodylate (pH 7.4) at 4°C overnight, and postfixed for 4 h in buffered 1% osmium tetroxide on ice. After rinsing with 0.1 mol/l sodium cacodylate (pH 7.4), specimens were dehydrated in a graded series of ethanol and embedded in LR White resin (London Resin Company, Reading, UK). Polymerization was achieved in gelatin capsules at 60°C for 48 h. Ultrathin sections of the specimens were cut with a diamond knife on a Leica Ultracut UCT ultramicrotome and placed on formvar-coated copper grids. Sections were stained with uranyl acetate and lead citrate and analyzed using a Philips CM10 TEM (Amsterdam, The Netherlands).

Statistical analysis
For all experiments, differences of data sets were considered statistically significant when *P*-values were lower than 0.05, if not

otherwise specified. Statistical comparisons were made using the two-tailed Student's *t*-test. Asterisks are used throughout the manuscript to specify statistical significance in comparison with the TCZ-treated groups (Figure 2 and 3b) or the IRI groups (Figure 5–7).

DISCLOSURE
All the authors declared no competing interests.

SUPPLEMENTARY MATERIAL
Figure S1. The tubular cell line TKPTS is protected from necroptosis by knockdown of RIP1.
Figure S2. Absence of cleaved caspase-3 in necroptotic TKPTS cells.
Figure S3. Knockdown of Rip3 protects the glomerular endothelial cell line glEND from necroptosis.
Figure S4. A human podocyte cell line is insensitive to both apoptosis and necroptosis.
Figure S5. Visualization of necroptotic hallmarks in tubular cells after renal ischemia/reperfusion.
Figure S6. The inactive derivative of Nec-1 (Nec-1i) does not protect from ischemia/reperfusion injury.
Supplementary material is linked to the online version of the paper at http://www.nature.com/ki

REFERENCES
1. Holler N, Zaru R, Micheau O *et al.* Fas triggers an alternative, caspase-8-independent cell death pathway using the kinase RIP as effector molecule. *Nat Immunol* 2000; **1**: 489–495.
2. Hotchkiss RS, Strasser A, McDunn JE *et al.* Cell death. *N Engl J Med* 2009; **361**: 1570–1583.
3. Krammer PH, Arnold R, Lavrik IN. Life and death in peripheral T cells. *Nat Rev Immunol* 2007; **7**: 532–542.
4. Linkermann A, Qian J, Janssen O. Slowly getting a clue on CD95 ligand biology. *Biochem Pharmacol* 2003; **66**: 1417–1426.
5. Hymowitz SG, Dixit VM. Unleashing cell death: the Fas-FADD complex. *Nat Struct Mol Biol* 2010; **17**: 1289–1290.
6. Tinel A, Tschopp J. The PIDDosome, a protein complex implicated in activation of caspase-2 in response to genotoxic stress. *Science* 2004; **304**: 843–846.
7. Tait SW, Green DR. Mitochondria and cell death: outer membrane permeabilization and beyond. *Nat Rev Mol Cell Biol* 2010; **11**: 621–632.
8. Callus BA, Vaux DL. Caspase inhibitors: viral, cellular and chemical. *Cell Death Differ* 2007; **14**: 73–78.
9. Krautwald S, Ziegler E, Rolver L *et al.* Effective blockage of both the extrinsic and intrinsic pathways of apoptosis in mice by TAT-crmA. *J Biol Chem* 2010; **285**: 19997–20005.
10. Cho YS, Challa S, Moquin D *et al.* Phosphorylation-driven assembly of the RIP1-RIP3 complex regulates programmed necrosis and virus-induced inflammation. *Cell* 2009; **137**: 1112–1123.
11. He S, Wang L, Miao L *et al.* Receptor interacting protein kinase-3 determines cellular necrotic response to TNF-alpha. *Cell* 2009; **137**: 1100–1111.
12. Zhang DW, Shao J, Lin J *et al.* RIP3, an energy metabolism regulator that switches TNF-induced cell death from apoptosis to necrosis. *Science* 2009; **325**: 332–336.
13. Challa S, Chan FK. Going up in flames: necrotic cell injury and inflammatory diseases. *Cell Mol Life Sci* 2010; **67**: 3241–3253.
14. Christofferson DE, Yuan J. Necroptosis as an alternative form of programmed cell death. *Curr Opin Cell Biol* 2010; **22**: 263–268.
15. Declercq W, Vanden Berghe T, Vandenabeele P. RIP kinases at the crossroads of cell death and survival. *Cell* 2009; **138**: 229–232.
16. Vandenabeele P, Galluzzi L, Vanden Berghe T *et al.* Molecular mechanisms of necroptosis: an ordered cellular explosion. *Nat Rev Mol Cell Biol* 2010; **11**: 700–714.
17. Degterev A, Huang Z, Boyce M *et al.* Chemical inhibitor of nonapoptotic cell death with therapeutic potential for ischemic brain injury. *Nat Chem Biol* 2005; **1**: 112–119.
18. Degterev A, Hitomi J, Germscheid M *et al.* Identification of RIP1 kinase as a specific cellular target of necrostatins. *Nat Chem Biol* 2008; **4**: 313–321.
19. Ch'en IL, Beisner DR, Degterev A *et al.* Antigen-mediated T cell expansion regulated by parallel pathways of death. *Proc Natl Acad Sci USA* 2008; **105**: 17463–17468.
20. Ch'en IL, Tsau JS, Molkentin JD *et al.* Mechanisms of necroptosis in T cells. *J Exp Med* 2011; **208**: 633–641.
21. Trichonas G, Murakami Y, Thanos A *et al.* Receptor interacting protein kinases mediate retinal detachment-induced photoreceptor necrosis and compensate for inhibition of apoptosis. *Proc Natl Acad Sci USA* 2010; **107**: 21695–21700.
22. Northington FJ, Chavez-Valdez R, Graham EM *et al.* Necrostatin decreases oxidative damage, inflammation, and injury after neonatal HI. *J Cereb Blood Flow Metab* 2011; **31**: 178–189.
23. Smith CC, Davidson SM, Lim SY *et al.* Necrostatin: a potentially novel cardioprotective agent? *Cardiovasc Drugs Ther* 2007; **21**: 227–233.
24. Varfolomeev EE, Schuchmann M, Luria V *et al.* Targeted disruption of the mouse Caspase 8 gene ablates cell death induction by the TNF receptors, Fas/Apo1, and DR3 and is lethal prenatally. *Immunity* 1998; **9**: 267–276.
25. Kaiser WJ, Upton JW, Long AB *et al.* RIP3 mediates the embryonic lethality of caspase-8-deficient mice. *Nature* 2011; **471**: 368–372.
26. Oberst A, Dillon CP, Weinlich R *et al.* Catalytic activity of the caspase-8-FLIP(L) complex inhibits RIPK3-dependent necrosis. *Nature* 2011; **471**: 363–367.
27. Welz PS, Wullaert A, Vlantis K *et al.* FADD prevents RIP3-mediated epithelial cell necrosis and chronic intestinal inflammation. *Nature* 2011; **477**: 330–334.
28. Sharfuddin AA, Molitoris BA. Pathophysiology of ischemic acute kidney injury. *Nat Rev Nephrol* 2011; **7**: 189–200.
29. Zhang ZX, Wang S, Huang X *et al.* NK cells induce apoptosis in tubular epithelial cells and contribute to renal ischemia-reperfusion injury. *J Immunol* 2008; **181**: 7489–7498.
30. Day YJ, Huang L, Ye H *et al.* Renal ischemia-reperfusion injury and adenosine 2A receptor-mediated tissue protection: the role of CD4+ T cells and IFN-gamma. *J Immunol* 2006; **176**: 3108–3114.
31. Day YJ, Huang L, Ye H *et al.* Renal ischemia-reperfusion injury and adenosine 2A receptor-mediated tissue protection: role of macrophages. *Am J Physiol Renal Physiol* 2005; **288**: F722–F731.
32. Burne MJ, Daniels F, El GA *et al.* Identification of the CD4(+) T cell as a major pathogenic factor in ischemic acute renal failure. *J Clin Invest* 2001; **108**: 1283–1290.
33. Nogae S, Miyazaki M, Kobayashi N *et al.* Induction of apoptosis in ischemia-reperfusion model of mouse kidney: possible involvement of Fas. *J Am Soc Nephrol* 1998; **9**: 620–631.
34. Ortiz A, Lorz C, Egido J. The Fas ligand/Fas system in renal injury. *Nephrol Dial Transplant* 1999; **14**: 1831–1834.
35. Ko GJ, Jang HR, Huang Y *et al.* Blocking Fas ligand on leukocytes attenuates kidney ischemia-reperfusion injury. *J Am Soc Nephrol* 2011; **22**: 732–742.
36. Zhang H, Zhou X, McQuade T *et al.* Functional complementation between FADD and RIP1 in embryos and lymphocytes. *Nature* 2011; **471**: 373–376.
37. Linkermann A, Himmerkus N, Rolver L *et al.* Renal tubular Fas ligand mediates fratricide in cisplatin-induced acute kidney failure. *Kidney Int* 2011; **79**: 169–178.
38. Daemen MA, van 't Veer C, Denecker G *et al.* Inhibition of apoptosis induced by ischemia-reperfusion prevents inflammation. *J Clin Invest* 1999; **104**: 541–549.
39. Schumer M, Colombel MC, Sawczuk IS *et al.* Morphologic, biochemical, and molecular evidence of apoptosis during the reperfusion phase after brief periods of renal ischemia. *Am J Pathol* 1992; **140**: 831–838.
40. Linkermann A, Qian J, Lettau M *et al.* Considering Fas ligand as a target for therapy. *Expert Opin Ther Targets* 2005; **9**: 119–134.
41. van Raam BJ, Salvesen GS. Proliferative vs. apoptotic functions of caspase-8 Hetero or homo: the caspase-8 dimer controls cell fate. *Biochim Biophys Acta* 2011; **1824**: 113–122.
42. Zhang DW, Zheng M, Zhao J *et al.* Multiple death pathways in TNF-treated fibroblasts. *Cell Res* 2011; **21**: 368–371.

43. Burne MJ, Elghandour A, Haq M *et al*. IL-1 and TNF independent pathways mediate ICAM-1/VCAM-1 up-regulation in ischemia reperfusion injury. *J Leukoc Biol* 2001; **70**: 192–198.

44. Kuida K, Zheng TS, Na S *et al*. Decreased apoptosis in the brain and premature lethality in CPP32-deficient mice. *Nature* 1996; **384**: 368–372.

45. Yeh WC, Pompa JL, McCurrach ME *et al*. FADD: essential for embryo development and signaling from some, but not all, inducers of apoptosis. *Science* 1998; **279**: 1954–1958.

46. Zhang J, Cado D, Chen A *et al*. Fas-mediated apoptosis and activation-induced T-cell proliferation are defective in mice lacking FADD/Mort1. *Nature* 1998; **392**: 296–300.

47. Galluzzi L, Aaronson SA, Abrams J *et al*. Guidelines for the use and interpretation of assays for monitoring cell death in higher eukaryotes. *Cell Death Differ* 2009; **16**: 1093–1107.

48. Kaushal GP, Basnakian AG, Shah SV. Apoptotic pathways in ischemic acute renal failure. *Kidney Int* 2004; **66**: 500–506.

49. Devalaraja-Narashimha K, Diener AM, Padanilam BJ. Cyclophilin D gene ablation protects mice from ischemic renal injury. *Am J Physiol Renal Physiol* 2009; **297**: F749–F759.

50. Bertrand MJ, Vandenabeele P. The ripoptosome: death decision in the cytosol. *Mol Cell* 2011; **43**: 323–325.

51. Tenev T, Bianchi K, Darding M *et al*. The Ripoptosome, a signaling platform that assembles in response to genotoxic stress and loss of IAPs. *Mol Cell* 2011; **43**: 432–448.

52. Feoktistova M, Geserick P, Kellert B *et al*. cIAPs block ripoptosome formation, a RIP1/caspase-8 containing intracellular cell death complex differentially regulated by cFLIP isoforms. *Mol Cell* 2011; **43**: 449–463.

53. Arany I, Megyesi JK, Kaneto H *et al*. Activation of ERK or inhibition of JNK ameliorates H(2)O(2) cytotoxicity in mouse renal proximal tubule cells. *Kidney Int* 2004; **65**: 1231–1239.

54. Wu H, Chen G, Wyburn KR *et al*. TLR4 activation mediates kidney ischemia/reperfusion injury. *J Clin Invest* 2007; **117**: 2847–2859.

Supplementary Material to

RIP1-mediated necroptosis essentially contributes to renal ischemia/reperfusion injury

Running headline: Necroptosis in renal IRI

Andreas Linkermann[1], Jan H. Bräsen[2], Nina Himmerkus[3], Shuya Liu[4],

Tobias B. Huber[4], Ulrich Kunzendorf[1] and Stefan Krautwald[1]

[1]Division of Nephrology and Hypertension, Christian-Albrechts-University, Kiel, Germany

[2]Institute for Pathology, Christian-Albrechts-University, Kiel, Germany

[3]Institute of Physiology, Christian-Albrechts-University, Kiel, Germany

[4]Renal Division, University Hospital Freiburg, Germany

SUPPLEMENTARY METHODS

Equal amounts of protein (20 µg/lane) were resolved on SDS-PAGE gels and transferred to nitrocellulose membranes (Amersham Biosciences, Freiburg, Germany). Western blots were performed using a polyclonal anti-cleaved caspase-3 antibody (Asp-175), (New England Biolabs) and a corresponding secondary horseradish peroxidase-linked anti-mouse (Promega, Mannheim, Germany). Immune complexes were visualized by enhanced chemiluminescence (Amersham Biosciences).

Human immortalized podocytes were cultivated as described previously.[1] Briefly, cells were grown in RPMI 1640 medium supplemented with L-Glutamine, insulin, transferrin, sodiumselenite (Roche Diagnostics, Mannheim, Germany), sodium pyruvate, MEM non-essential amino acids, HEPES (Invitrogen, Karlsruhe, Germany) and 10% fetal calf serum at the permissive temperature of 33° C in 5% CO_2 to cell confluence of 60 - 80%. Subsequently, the cells were shifted to the nonpermissive temperature of 37° C (5% CO_2) to allow terminal differentiation for 10 to 14 days.

RNA interference: The non-targeting small interfering RNA (siRNA) oligonucleotides and siRNA oligonucleotide targeting mouse RIP1 or RIP3 (ON-TARGETplus SMARTpool) were obtained from Dharmacon (Thermo Fisher Scientific, Epsom, UK). All siRNA (100 nM) were transfected 48 hrs prior to TCZ stimulation into TKPTS cells or glEND cells using the DharmaFECT 4 Transfection Reagents according to manufacturer's protocol.

SUPPLEMENTARY REFERENCES

1. Saleem MA, O'Hare MJ, Reiser J *et al.*: A conditionally immortalized human podocyte cell line demonstrating nephrin and podocin expression. *J Am Soc Nephrol* 13:630-638, 2002

SUPPLEMENTARY FIGURE LEGENDS

Supplementary Figure 1. The tubular cell line TKPTS is protected from necroptosis by knockdown of RIP1.

Knockdown of RIP1 in TKPTS cells was performed as described in SUPPLEMENTARY METHODS for 48 hours followed by combined treatment with TNFα/CHX/zVAD (TCZ) for additional 24 hours. Annexin V positivity was measured by FACS analysis.

Supplementary Figure 2. Absence of cleaved caspase-3 in necroptotic TKPTS cells.

Jurkat cells or TKPTS cells were treated either with vehicle or TNFα/CHX in the presence or absence of the pan-caspase-inhibitor zVAD for indicated times. No cleavage products of caspase-3 could be detected in TKPTS cells in any of these settings, demonstrating that this form of programmed cell death is caspase-independent.

Supplementary Figure 3. Knockdown of RIP3 protects the glomerular endothelial cell line glEND from necroptosis.

Knockdown of RIP3 in glEND cells was performed as described in SUPPLEMENTARY METHODS for 48 hours followed by combined treatment with TNFα/CHX/zVAD (TCZ) for additional 24 hours. Accordingly, Annexin V positivity was measured by FACS analysis.

Supplementary Figure 4. A human podocyte cell line is insensitive to both apoptosis and necroptosis.

A human podocyte cell line was left untreated or treated with 200 ng/ml TNFα, 200 ng/ml TNFα + 2 µg/ml CHX and 200 ng/ml TNFα + 2 µg/ml CHX + 25 µM zVAD as indicated. Annexin V positivity was measured 24 hours later by FACS analysis. Data from two independent experiments are shown. Note that TNFα stimulation in these cells did not lead to any detectable levels of phosphatidylserine exposure to the extracellular environment.

Supplementary Figure 5. Visualization of necroptotic hallmarks in tubular cells after renal ischemia/reperfusion.

(A - C) Experimental settings are identical to Fig. 5C (untreated, IR, IR + Nec-1). Nuclear swelling, loss of mitochondria and loss of cell organelle content are hallmarks of IRI. Application of Nec-1 appears to prevent loss of mitochondria in the basolateral compartment. Note the frequency of mitochondria that show outer membrane rupture and loss of christae formation in B. IR-induced nuclear swelling and loss of nuclear ultrastructural features are prevented by addition of Nec-1. Magnification is 19.000-fold and scale bar represents 500 nm.

Supplementary Figure 6. The inactive derivative of Nec-1 (Nec-1i) does not protect from ischemia/reperfusion injury.

6 - 8 week old male C57BL/6N mice underwent sham surgery or underwent 30 minutes of bilateral renal pedicle clipping in the presence of 200 µl PBS or 1.65 mg/kg body weight Nec-1i in equal volume as indicated.
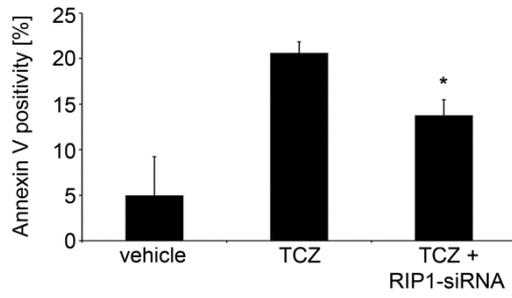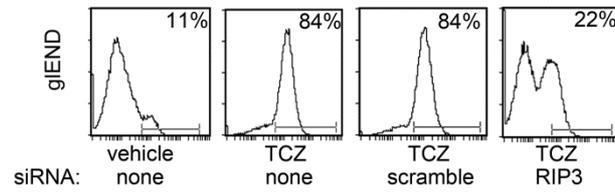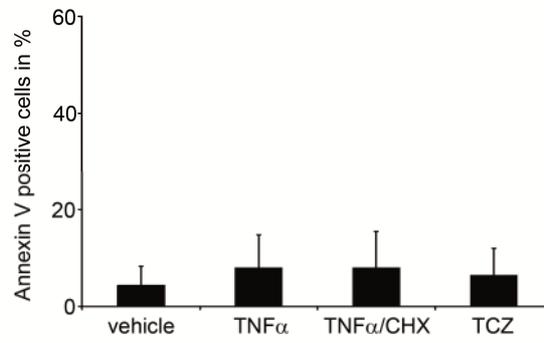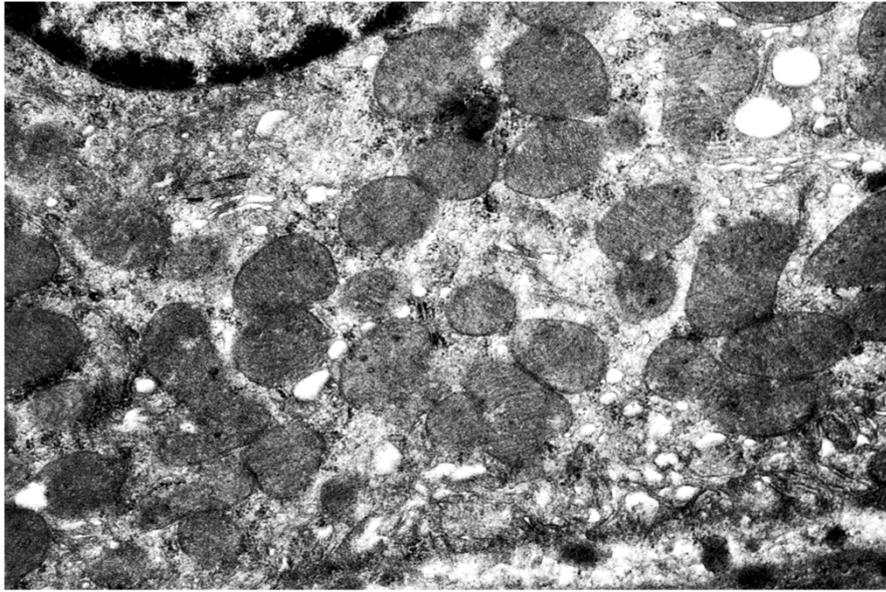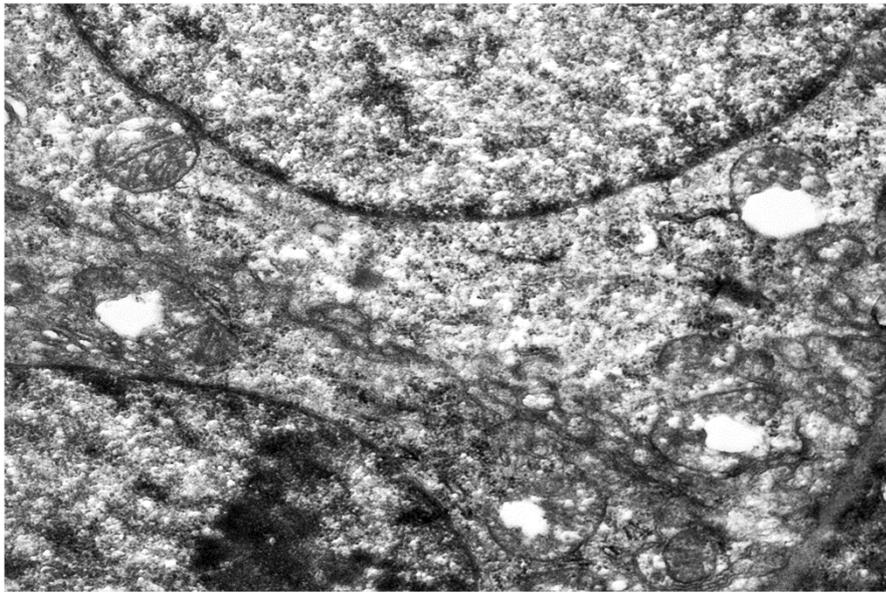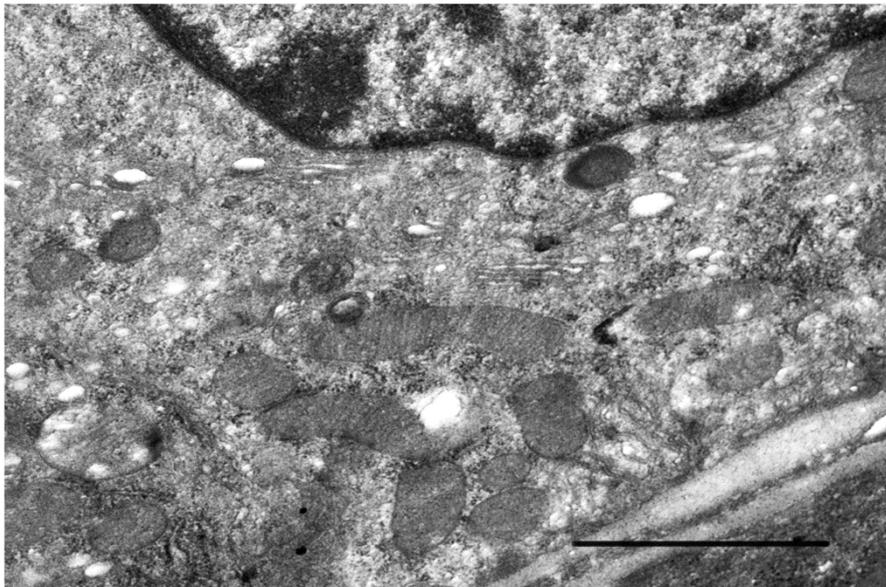
Fig. S1
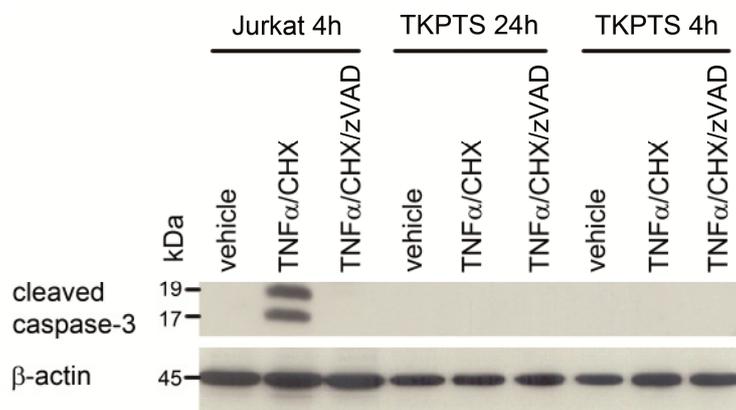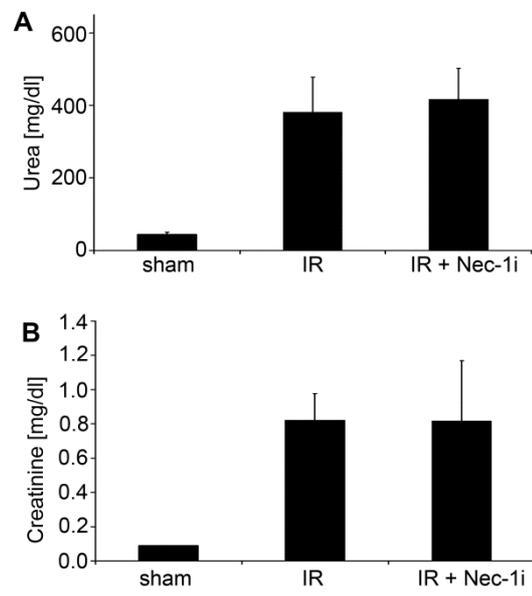

Fig. S2

Fig. S3

Fig. S4

A

untreated

B

IR

C

IR + Nec-1

Fig. S5

Fig. S6